Broadband Low-power Optical Modulator Based on Electro-optic Polymer Infiltrated Silicon Slot Photonic Crystal Waveguide

[1]Xingyu Zhang*, [2]Amir Hosseini, [2]Harish Subbaraman, [3]Jingdong Luo, [3]Alex K.-Y. Jen, [4]Robert L. Nelson, and [1]Ray T. Chen*

[1]Microelectronics Research Center, Electrical and Computer Engineering Department, University of Texas at Austin, Austin, TX, 78758, USA
[2]Omega Optics, Inc, 8500 Shoal Creek Blvd, Bldg 4, Ste 200, Austin, TX 78757, USA
[3]Department of Materials Science and Engineering, University of Washington, Seattle, Washington 98195, USA
[4]Air Force Research Laboratory at Wright Patterson, Dayton, Ohio 45433, USA
**Corresponding author: xzhang@utexas.edu, raychen@uts.cc.utexas.edu, Tel:512- 471-4349, Fax: +1-512-471-8575*

Abstract: We demonstrate a broadband, low-dispersion, sub-volt and compact optical modulator based on electro-optic polymer infiltrated silicon slot photonic crystal waveguide. Modulation up to 43GHz, $V_\pi \times L=0.282V \times mm$, and optical bandwidth of 8nm are experimentally demonstrated.
OCIS codes: (230.4110) Modulators; (130.5296) Photonic crystal waveguides; (250.2080) Polymer active devices.

The combination of silicon photonics and electro-optic (EO) polymers has shown to enable compact and high-performance hybrid integrated optical modulators [1]. Silicon photonic crystal waveguides (PCWs) infiltrated with EO polymers can further enhance modulation performance and reduce device size due to slow-light effect. Here we report an MZI modulator based on band-engineered slot PCW refilled with EO polymer [SEO125, EO coefficient (r_{33}) of 120pm/V]. A small $V_\pi \times L=0.282V \times mm$ is demonstrated, corresponding to a record-high effective in-device r_{33} of 1230pm/V. The modulation is demonstrated to be up to 43GHz. The optical bandwidth is measured to be 8nm.

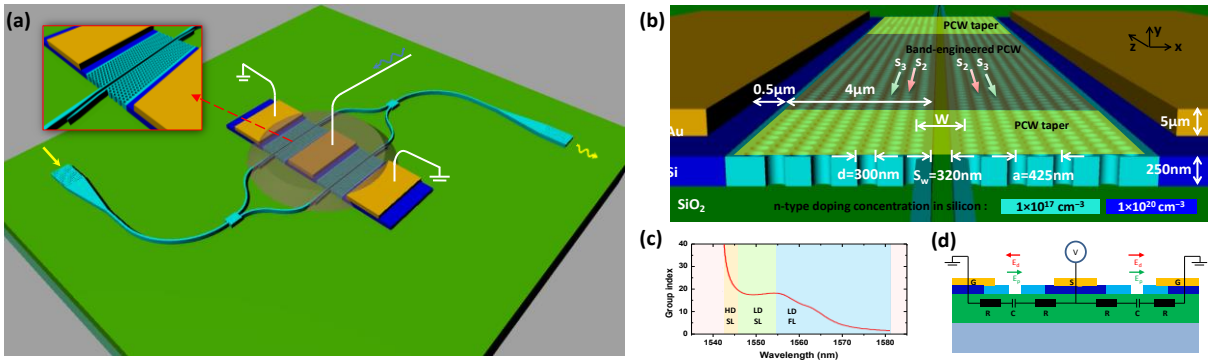

Fig. 1. (a) Schematic of the EO polymer infiltrated silicon slot PCW MZI modulator. (b) A tilted view of the slot PCW on one arm of the MZI, showing the device dimension, 2-level doping concentration, PCW taper region and band-engineered PCW region. (c) Simulate result of engineered group index as a function of wavelength, showing 8nm low-dispersion slow-light wavelength region. The inset shows the mode profile of the EO polymer infiltrated slot PCW. HD SL: high-dispersion slow-light; LD SL: low-dispersion slow-light; LD FL: low-dispersion fast-light. (d) Equivalent circuit of the MZI modulator in a push-pull configuration.

Fig. 1 (a) shows a schematic of our modulator on SOI substrate (250nm Si, 3μm oxide). The 300 μm-long PCW section is band-engineered by lateral shifting of the second and the third rows on the two sides of the slot [indicated by s_2 and s_3 in Fig. 1 (b)] and by varying the center-to-center distance between two rows adjacent to the slot [W in Fig. 1 (b)]. For lattice constant, a=425nm, it is found that with a hole diameter d=300nm, s_2=-85nm, s_3=85nm, S_w=320nm, and W=1.54($\sqrt{3}$)a, a group index ($n_g=c/v_g$) of 20.4 (±10%) over 8.2nm optical bandwidth is achieved as shown in Fig. 1 (c) [2]. To reduce n_g mismatch between slot waveguides (n_g~3) and slot PCWs (n_g~20.4), PCW tapers are used to serve as a smooth transmission of n_g [3]. The input and output strip waveguides are connected to the slot PCW with adiabatic strip-to-slot mode converters [4]. In addition, to reduce RC time delay and thus increase the RF bandwidth of the modulator, the silicon PCW is selectively implanted by n-type dopant with concentration of 1×10^{20}cm^{-3} and 1×10^{17}cm^{-3}, as shown in Figs.1 (a) and (b) [5]. The equivalent circuit is shown in Fig. 1 (d).

The device is fabricated using e-beam lithography and RIE in a single patterning/etching step, and then doped by photolithography and ion implantation, while gold electrodes are patterned by photolithography, e-beam evaporation and lift-off process. Then the EO polymer is formulated [6] and infiltrated into the slot and holes of silicon PCW region by spincoating. Next, the device is poled by an electric field of 110V/μm in a push-pull configuration at 150 ℃. During the poling process, the maximum leakage current density is monitored to be 5.5A/m^2, which is comparable to that measured in a thin film configuration (2.4A/m^2 in data sheet). This test result shows that the

320nm-wide slot dramatically reduces the poling leakage current through the silicon–polymer interface and thus significantly increase the EO coefficient of the poled polymer [2].

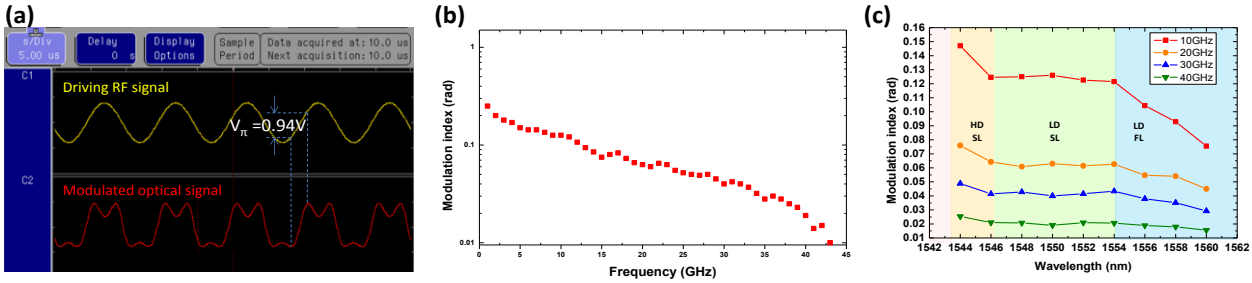

Fig. 2. (a) Transfer function in low frequency modulation test. (b) Measured modulation index as a function of frequency up to 43GHz. (c) Measured modulation index over a range of wavelength, at different high modulation frequencies. The modulation index is nearly constant over the 8nm low-dispersion slow-light region.

Low-frequency modulation test is first implemented. TE-polarized light from a tunable laser source (1550nm) is coupled into and out of the device through grating couplers. The modulator is biased at the 3dB point and driven by a 100KHz sinusoidal RF wave with a peak-to-peak voltage of 1.5V, as shown in Fig. 1 (d). The modulated output optical signal is sent to a photodetector and then displayed on a digital oscilloscope. As shown in Fig. 2 (a), an over-modulation is observed on the output optical waveform [6], and the V_π of the modulator is measured to be 0.94V. The figure of merit of the modulator is achieved to be $V_\pi \times L = 0.94\text{V} \times 300\mu\text{m} = 0.282\text{V} \times \text{mm}$. A record-high effective in-device r_{33} is then calculated as

$$r_{33-effective} = \frac{\lambda S_w}{n^3 V_\pi \sigma L} = 1230\text{pm/V} \quad (1)$$

where, λ=1.55μm, S_w=320nm, n=1.63, L=300μm, σ=0.33 (confinement factor in the slot) calculated by simulation. This extraordinarily high r_{33} value originates from the enhancing effects of slow light, an improved poling efficiency by widening slot width (320nm), and the increased percentage of voltage drop across the slot due to silicon doping. The actual in-device r_{33} excluding the slow-light effect is also estimated to be 98pm/V [2], which is the highest poling efficiency demonstrated in an EO polymer infiltrated slot, to the best of our knowledge.

Next, a small signal modulation test at high frequencies is performed. RF driving signal of 0.16V at GHz frequency regime is provided by a network analyzer, and applied onto the electrodes of the modulator via a GSG picoprobe. The optical output of the modulator is directly connected to the optical spectrum analyzer (OSA), and the transmission spectrum is measured. Sidebands together with the main peak are observed in the transmission spectrum, and their powers are used to calculate the phase modulation index [7]. The obtained modulation index (η) as a function of frequency is plotted in Fig. 2 (b). It can be seen that high frequency modulation is achieved up to 43GHz, until the sideband signals are buried under the noise floor in which case the modulation index is about 0.01.

Finally, the wavelength of the laser input is tuned from 1544nm to 1560nm, while all other testing conditions are fixed. The modulation index over this wavelength range is measured at 10GHz, 20GHz, 30GHz, and 40GHz, and the results are plotted in Fig. 2 (c). It can be seen that, at each modulation frequency, the measured modulation index has a small variation of ±3.5% from 1546nm to 1554nm, because the n_g is engineered to be almost constant over this low-dispersion slow-light (LD SL) wavelength region which can be seen in Fig. 1(c). This 8nm-wide optical bandwidth provides the modulator some potential applications such as wavelength division multiplexing. In our future work, this device can be extended as an antenna-coupled modulator for RF sensing [5] and light trapping [8].

Reference

[1] X. Zhang, A. Hosseini, X. Lin, H. Subbaraman, and R. T. Chen, "Polymer-based Hybrid Integrated Photonic Devices for Silicon On-chip Modulation and Board-level Optical Interconnects," *IEEE Journal of Selected Topics in Quantum Electronics*, vol. 16, p. 3401115, 2013.

[2] X. Zhang, A. Hosseini, S. Chakravarty, J. Luo, A. K.-Y. Jen, and R. T. Chen, "Wide optical spectrum range, subvolt, compact modulator based on an electro-optic polymer refilled silicon slot photonic crystal waveguide," *Optics letters*, vol. 38, pp. 4931-4934, 2013.

[3] A. Hosseini, X. Xu, D. N. Kwong, H. Subbaraman, W. Jiang, and R. T. Chen, "On the role of evanescent modes and group index tapering in slow light photonic crystal waveguide coupling efficiency," *Applied Physics Letters*, vol. 98, pp. 031107-031107-3, 2011.

[4] X. Zhang, H. Subbaraman, A. Hosseini, and R. T. Chen, "Highly efficient mode converter for coupling light into wide slot photonic crystal waveguide," *Optics Express*, vol. 22, pp. 20678-20690, 2014.

[5] X. Zhang, A. Hosseini, H. Subbaraman, S. Wang, Q. Zhan, J. Luo, A. Jen, and R. Chen, "Integrated Photonic Electromagnetic Field Sensor Based on Broadband Bowtie Antenna Coupled Silicon Organic Hybrid Modulator," *Lightwave Technology, Journal of*, vol. 32, p. 3774, 2014.

[6] X. Zhang, B. Lee, C.-y. Lin, A. X. Wang, A. Hosseini, and R. T. Chen, "Highly Linear Broadband Optical Modulator Based on Electro-Optic Polymer," *Photonics Journal, IEEE*, vol. 4, pp. 2214-2228, 2012.

[7] L. Alloatti, D. Korn, R. Palmer, D. Hillerkuss, J. Li, A. Barklund, R. Dinu, J. Wieland, M. Fournier, and J. Fedeli, "42.7 Gbit/s electro-optic modulator in silicon technology," *Optics Express*, vol. 19, pp. 11841-11851, 2011.

[8] X. Li, P. Li, D. Hu, D. Schaadt, and E. Yu, "Angular dependence of light trapping in In0. 3Ga0. 7As/GaAs quantum-well solar cells," *Journal of Applied Physics*, vol. 115, p. 044303, 2014.